Desalination and Water Treatment
www.deswater.com

doi: 10.1080/19443994.2015.1055808

57 (2016) 13091–13105
June

Taylor & Francis
Taylor & Francis Group

Sorption of cobalt(II) from an aqueous medium using Amberlite 200C and Dowex 88 resins: Equilibrium and kinetic studies

Y. Aşçı*, Ş. Kaya

Department of Chemical Engineering, Eskişehir Osmangazi University, Batı Meşelik, Eskişehir, Turkey, Tel. +90 545 7298873; Fax: +90 222 234 9718; email: yelizbal@ogu.edu.tr (Y. Aşçı), Tel. +90 546 2484826; email: sefikakaya@ogu.edu.tr (Ş. Kaya)

Received 8 July 2014; Accepted 23 May 2015

ABSTRACT

Cobalt is a toxic heavy metal found in various industrial wastewaters. In this study, the sorption mechanisms of Co(II) onto Amberlite 200C and Dowex 88 resins were investigated using batch reactors. The removal of Co(II) was examined by varying experimental conditions, such as the solution pH, sorbent dose, and temperature. The most effective pH range for cobalt removal was pH 4–8 for both resins. Langmuir, Freundlich, Redlich–Peterson, and Temkin models were applied to describe equilibrium isotherms. The sorption of Co(II) on the resins followed pseudo-second-order kinetics, and thermodynamic data indicated an endothermic and spontaneous process. ΔG° decreased with increasing temperature, indicating that the sorption process of Co(II) on both resins was more favorable at high temperatures. Desorption studies were conducted using various reagents. For both resins, the maximum percent of metal ion desorption was reached when 2 M H_2SO_4 was used as the reagent.

Keywords: Resin; Cobalt; Sorption; Desorption; Activation energy

1. Introduction

Rapid industrialization and the increasing world population have contributed to heavy metal pollution [1]. Heavy metals can be distinguished from other pollutants, because they are not biodegradable and can accumulate in nature. Several heavy metals are significantly toxic to humans and the environment, including antimony (Sb), chromium (Cr), cobalt (Co), copper (Cu), lead (Pb), manganese (Mn), mercury (Hg), cadmium (Cd), etc. [2,3].

Cobalt is an oligo element that is essential for human health because it is part of vitamin B12. Additionally, cobalt has numerous applications in industrial and medicinal fields. Cobalt and cobalt salts are used in nuclear medicines, enamels, semiconductors, grinding wheels, varnishes, paints (including paints for glass and porcelain, hygrometers, and electroplaters), and for manufacturing vitamin B12. Cobalt is also used as a foam stabilizer in beer, as a drier for lacquers, and as a catalyst for organic chemical reactions. However, high concentrations of Co(II) are detrimental to human health and can cause paralysis, diarrhea, lung irritation, and bone defects [4–6]. If cobalt is present at concentrations greater than permissible limits, it can result in toxic effects, such as neurotoxicological disorders, genotoxicity, carcinogenecity, cardiomyopathy, and bronchial asthma. The standard levels of cobalt in drinking and irrigation water are 0.002 and 0.05 mg/L, respectively [7–9].

---

*Corresponding author.

1944-3994/1944-3986

Thus, the removal of cobalt ions from wastewater is extremely important for maintaining cobalt's economic value because it is frequently present in wastewater from industrial facilities.

Various strategies have been used to remove cobalt ions from wastewaters, such as chemical precipitation [10,11], membrane separation [12,13], electrocoagulation [14], and sorption [6,15,16]. Sorption, which is used here as a general term that includes ion exchange and adsorption mechanisms, is a common treatment method used in many water and wastewater treatment systems. Sorption is also used to regulate chemical transport in aquatic systems. Among these physico-chemical treatment processes, ion-exchange processes are highly effective, cost efficient, and easy to operate. Furthermore, ion-exchange process is particularly effective and is commonly applied for treating water that contains low concentrations of heavy metals [17]. Additionally, related sludge production and disposal are minimal during ion exchange [9]. However, the selection of the resins used for ion exchange is very important and should be based on the cost, exchange capacity, stability, selectivity, and regeneration capacity of the resins. In previous studies, cation-exchange resins, including Dowex M 4195R, Amberlite IRC 748R, Ionac SR-5R, Purolite S930R [18], IRN 77, SKN1 [4], and NKC-9 [19] resins, a modified magnetic chitosan chelating resin [6,20], and Lewatit MonoPlus SP 112 [21] resin, were used to remove Co (II) from aqueous solutions and wastewaters.

In this study, low-cost Amberlite 200C and Dowex 88 cation-exchange resins were used to remove cobalt ions from aqueous media. The main objective of this study was to investigate the sorption mechanisms of cobalt onto Amberlite 200C and Dowex 88 resins. To the best of our knowledge, few studies have been conducted regarding the sorption mechanisms and behavior of cobalt on these resins. Thus, kinetic, isotherm and thermodynamic analyses were performed. The effects of various system parameters, such as solution pH, resin dose, and temperature, were also studied. Moreover, the desorption of Co(II) from these resins was investigated, and the obtained results are discussed below.

2. Experimental

2.1. Resins

Two strong acid cation-exchange resins, Amberlite 200C and Dowex 88, were used in this study. Cation-exchange resins generally include bound sulfonic acid groups and occasionally include carboxylic, phosphonic, or phosphinic groups. Amberlite 200C and Dowex 88 resins are characterized by sulfonic acid functional groups. These groups are bound in a macroporous polystyrene matrix, and the resins are macroreticular (polyreticular). Consequently, the resins are more resistant to chemical oxidation and degradation due to mechanical, thermal, or osmotic shock than any other commercially available cation resin.

Amberlite 200C and Dowex 88 cation-exchange resins (sodium type) were purchased from Sigma-Aldrich. The physical properties of these two resins, as reported by the supplier, are shown in Table 1. Samples of each resin (20–30 g) were collected in glass beakers. Then, each resin was washed with distilled water to remove impurities before drying in an oven at 80˚C for 24 h. Finally, the resins were stored in a desiccator until further study.

2.2. Chemicals and instrumentations

Stock Co(II) solutions were prepared by dissolving $Co(NO_3)_2 \cdot 6H_2O$ in distillated water. The solution pH was adjusted to different values using dilute HNO_3 or NaOH (from Sigma Aldrich). The Co(II) ion concentration was determined using a flame atomic absorption spectrophotometer (Perkin Elmer model AA 400), and a Hanna Model pH meter was used to measure pH. Each sample was shaken using a Memmert constant temperature shaking water bath.

2.3. Sorption studies

2.3.1. Effects of pH

A 1,000 mg/L Co(II) stock solution was prepared by dissolving $Co(NO_3)_2 \cdot 6H_2O$ in distilled water. Next, 25-mL aliquots of the 100-mg/L metal ion solutions were added to 0.25 g of each resin in 50-mL centrifuge tubes. The pH values of the suspensions were adjusted to 2.0, 3.0, 4.0, 5.0, 6.0, 7.0, and 8.0. Then, the centrifuge tubes were agitated at 150 rpm for 240 min using a shaker at 25˚C. The tubes were centrifuged, and the cobalt concentrations in the resulting supernatant solutions were measured using flame atomic absorption spectroscopy. The amount of Co(II) sorbed by the resin (q_e) was calculated as follows:

$$q_e = \frac{(C_0 - C_e)V}{M} \tag{1}$$

where C_0 (mg/L) and C_e (mg/L) are the concentrations in the solution at time t = 0 and at equilibrium time t, V is the volume of the treatment solution (L), and M is the amount of sorbent added (g).

Table 1
Characteristics of the Amberlite 200C and Dowex 88 cation exchange resins

Characteristics	Amberlite 200C	Dowex 88
Ionic forms as shipped	Na^+	Na^+
Particle size	20–45 mesh	16–40 mesh
Matrix	Styrene divinylbenzene copolymer	Styrene divinylbenzene
Functional group	Sulfonic acid	Sulfonic acid
Total exchange capacity	1.7 eq/L	1.8 eq/L
Water retention capacity	46–52%	42–48%
pH	0–14	0–14
Maximum operating temperature	135°C	93°C

2.3.2. *Effect of resin dosage*

Next, 0.01, 0.025, 0.05, 0.075, 0.1, 0.25, 0.50, 0.75, and 1 g of each resin were added to 25 mL of the 100-mg/L metal ion solutions in 50-mL centrifuge tubes. The metal ion solutions were maintained at pH 5.7. The centrifuge tubes were agitated on a shaker at 150 rpm for 240 min at 25°C. The samples were then centrifuged, and the remaining concentration in the supernatant solution was analyzed.

2.3.3. *Equilibrium studies*

Sorption onto the resins was studied using 0.5 g of resin, 25 mL of solution at pH 5.7, and initial cobalt concentrations of 25, 50, 100, 150, 200, 250, 300, and 350 mg/L at 25°C. The solutions were shaken until equilibrium was reached. The experimental data obtained from this experiment were evaluated using Langmuir, Freundlich, Redlich–Peterson, and Temkin isotherm models.

2.3.4. *Kinetic and thermodynamic studies*

A fixed amount (0.5 g) of resin was added to a 25-mL sample with an initial cobalt concentration of 100 mg/L at pH 5.7, and then aliquots were taken at several time intervals (2, 5, 10, 15, 30, 45, 60, 90, 120, 150, 180, 240, 300, and 360 min) until the sorption equilibrium was reached to determine the kinetics and thermodynamics of sorption. These experiments were conducted at 25, 35, and 45°C, and the equilibrium values at 240 min for each temperature were used for the thermodynamic calculations.

2.4. *Statistical analyses from the isotherm and kinetic studies*

Each experiment was performed in duplicate, and averaged values were used for all analyses. The standard deviation of the metal uptake per gram of resin (S) was obtained using the Curve Expert 1.3 biological software computer program for isotherm studies, and the sum of square error (SSE) was calculated using Eq. (2) for kinetic studies [22].

$$\mathrm{SSE} = \sum_{i=1}^{N} (q_{\mathrm{e,cal}} - q_{\mathrm{e,exp}})^2 \tag{2}$$

$q_{\mathrm{e,cal}}$ is the uptake capacity of cobalt that was calculated using the kinetic models, $q_{\mathrm{e,exp}}$ is the experimental uptake capacity of cobalt, and N is the number of measurements. Smaller S and SSE values correspond with better curve fits.

2.5. *Desorption studies*

For batch desorption experiments, HCl, NaOH, HNO_3, and H_2SO_4 solutions were used at various concentrations. The Co(II)-loaded resin and eluent solutions with different concentrations were mixed in centrifuge tubes and shaken at 150 rpm for 240 min at 25°C. The metal concentrations in the solution were determined as described above.

3. Results and discussion

3.1. *Effects of pH*

To determine the optimum pH, the pH of the Co(II) solution was varied from 2 to 8. This pH range was chosen for the sorption study because cobalt hydroxide precipitation may occur above pH 8. The pH of the medium is critical in the sorption of metal ions from aqueous solutions. The sorption of a metal cation onto a sorbent depends on the nature of the sorbent surface and on the species distribution of the metal cation [4]. Figs. 1 and 2 shows the removal of Co(II) and the distribution of cobalt species against pH, respectively.

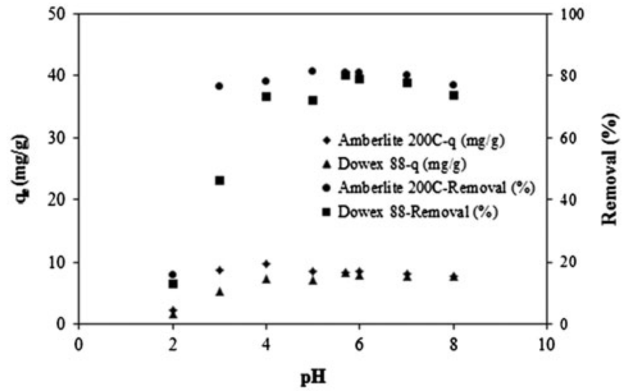

Fig. 1. Effects of pH on Co(II) sorption. Conditions: initial metal ion concentration: 100 mg/L; contact time: 240 min; sorbent dose: 10 g/L; temperature: 25˚C.

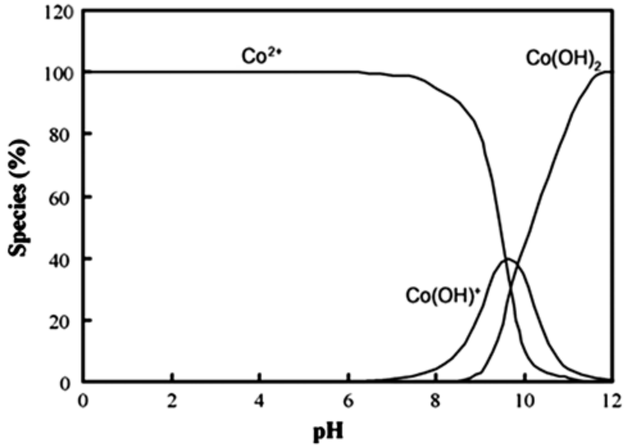

Fig. 2. Speciation diagram for Co(II) in aqueous solution [27].

As shown in Fig. 1, minimal cobalt sorption was observed at pH 2 for both resins. This sorption trend is likely due to competitive binding between Co(II) and hydrogen ions for sites on the resin surface [23]. Increasing the pH from 2 to 4 improved metal sorption potentially because the number of H^+ ions available to compete with the cationic metal ions to occupy the sorption sites decreased. In addition, increased sorption at higher pH values potentially resulted from the ionization of functional groups and increased the negative charge density on the resin surface, which could significantly improve the attractive force between the resin surface and cobalt cations. Increasing the pH from 4 to 8 resulted in a slight change in sorption. Hence, subsequent experiments were performed using a solution pH of 5.7 for both resins. Similar pH trends were observed using palygorskite [24], alginate beads [9], *Acacia nilotica* Leaf Carbon [25], natural hemp fibers, and sepiolite [16,26] for the removal of Co(II) ions.

As shown in Fig. 2, Co^{2+} remains dominant until the solution reaches a pH of approximately 8. This phenomenon may be attributed to the fact that cobalt species only exist in the divalent ionic form (*i.e.* Co^{2+}), which is favorable for removal by both resins. The precipitation of Co(II) was observed at a pH greater than 8.0. Although a quantitative description is not included in this study, it is anticipated that the variety of chemical forms of cobalt (*e.g.* $CoOH^+$, $Co(OH)_2$, *etc.*) at high pH may play a role in diminishing the overall Co(II)-removal efficiency [10,27,28].

3.2. Effects of resin dosage

The sorption capacity and percent removal of cobalt are plotted as functions of resin dosage in Fig. 3. Increasing the dosage of both resins increased the percentage removal of cobalt, and the maximum cobalt sorption was 99 and 98% when using 40 g/L Amberlite 200C and Dowex 88, respectively. Resin dosage is an important parameter because it determines the metal-retention capacity for a given initial metal concentration. As reported by several researchers, increasing the sorbent dosage provides a greater surface area or greater number ion-exchange sites for a fixed initial solute concentration [29]. However, the amount of cobalt sorbed per unit mass of the sorbent (q_e) decreased as the resin doses increased and then reached equilibrium. The decrease in the amount of cobalt sorbed with increasing sorbent dosage results from the presence of excess active sites on the resin compared with the quantity of cobalt present in the

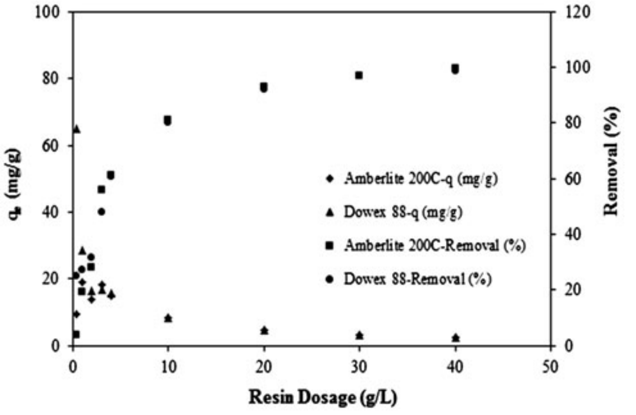

Fig. 3. Effects of resin dosage on Co(II) sorption. Conditions: initial metal ion concentration: 100 mg/L; contact time: 240 min; pH 5.7; temperature: 25˚C.

solution, whereas the number of available ion exchange sites increases as the amount of resin [4,29–31].

To visualize differences in the sorption capacity, 20 g/L of the sorbent dosage was used for further sorption studies.

3.3. Sorption isotherm

Generally, a sorption isotherm is the functional expression of the relationship between the sorbate distribution in the liquid and sorbent phases when the sorption process reaches an equilibrium state. Therefore, the sorption isotherm is important for understanding a sorption system. In this investigation, four isotherm equations, the Langmuir, Freundlich, Redlich Peterson, and Temkin isotherm equations, were used to describe the equilibrium characteristics of sorption [32].

The Langmuir model makes several assumptions, such as monolayer coverage and constant sorption energy. The Langmuir model represents one of the first theoretical treatments of non-linear sorption and has been successfully applied to a wide range of systems that exhibit limiting or maximum sorption capacities.

The Langmuir isotherm is commonly presented as follows [33,34]:

$$q_e = \frac{q_m K C_e}{1 + K C_e} \tag{3}$$

where C_e is the equilibrium concentration (mg/L), q_e is the amount sorbed at equilibrium (mg/g), K is the equilibrium constant related to the affinity of the binding sites for the metals or the Langmuir constant (L/mg), and q_m is the resin capacity (maximum possible number of metallic ions sorbed per unit mass of sorbent, mg/g) [4,29,35].

The Freundlich isotherm is an empirical equation that is often used to model sorption on heterogeneous surfaces that support sites with varying affinities. The Freundlich sorption isotherm relates the amounts of metal sorbed per unit mass of the sorbent (q_e) to the metal concentration at equilibrium (C_e) and can be described as follows:

$$q_e = K_f C_e^{1/n} \tag{4}$$

where K_f (mg/g)(L/mg)$^{1/n}$ and n are constants that represent the sorption capacity and intensity of sorption, respectively [29,36].

An empirical isotherm was also developed by Redlich and Peterson [37]. Redlich and Peterson incorporated the features of the Langmuir and Freundlich isotherms into a single equation as follows [38–40]:

$$q_e = \frac{K_R C_e}{1 + a_R C_e^{\beta}} \tag{5}$$

when $\beta = 1$, the Redlich–Peterson equation is reduced to the Langmuir equation. If $a_R {C_{eq}}^{\beta}$ is much greater than 1, then the equation becomes the Freundlich equation. If $a_R {C_{eq}}^{\beta}$ is much less than 1, which occurs at low concentrations, then the equation becomes a linear isotherm.

Temkin's isotherm explicitly considers sorbent–sorbate interactions. The sorption is characterized by a uniform distribution of binding energies, up to some maximum binding energy. The Temkin isotherm is represented by the following equation [2,32,41]:

$$q_e = B \cdot \ln K_T + B \cdot \ln C_e \tag{6}$$

$$B = R \cdot T / b_T \tag{7}$$

where b_T is the Temkin constant related to the heat of sorption (J/mol), K_T is the equilibrium binding constant that corresponds to the maximum binding energy (L/mg), R is the gas constant (8.314 J/mol K), and T is the absolute temperature (K).

All sorption model constants were estimated using a curve expert 1.3 biological software computer program. Furthermore, because of the three unknowns in the Redlich–Peterson model (a_R, K_R, and β), a minimization procedure was adopted to solve the above equation by maximizing the correlation coefficient between the theoretical data for q_e predicted from the above equation and the experimental data.

The Langmuir, Freundlich, Redlich–Peterson, and Temkin sorption isotherms obtained for the sorption of Co(II) ions are shown for both resins in Fig. 4(a) and (b). In all of the figures in which metal uptake equilibrium data are shown, the model profiles are presented as dashed lines and the experimentally obtained values are shown by symbols. The Langmuir, Freundlich, Redlich–Peterson, and Temkin constants and the standard errors of the estimate (S) and correlation coefficient (R^2) between the experimental and predicted values when using the models are given in Table 2.

When comparing the values of S and R^2 obtained from the sorption models, the fit between the experimental values and the predicted values was generally

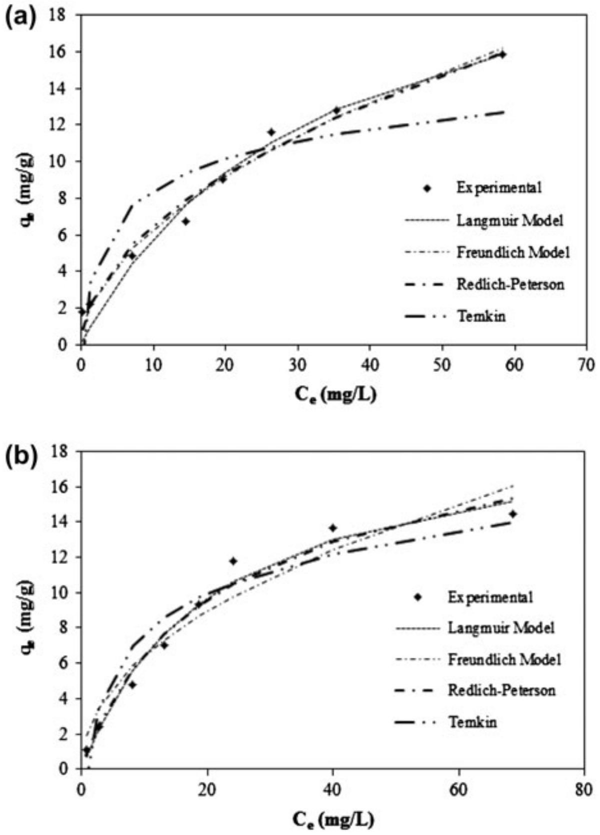

Fig. 4. Isotherm plots for the sorption of Co(II) on Amberlite 200C (a) and Dowex 88 (b). Conditions: contact time: 240 min; sorbent dose: 20 g/L; pH 5.7; temperature: 25˚C.

reasonable for all models of Co(II) sorption onto Dowex 88. However, the Langmuir model seems to best represent the measured sorption data. By contrast, the Freundlich and Redlich–Peterson models showed the best fits for of the sorption of Co(II) onto Amberlite 200C among the four examined models. However, the Temkin-type model failed to describe the sorption results and the $a_R C_e^{\beta}$ value was much greater than 1. This result indicates that the sorption isotherms for the metal concentrations studied were best described by the Freundlich model.

The value of the Freundlich sorption constant (n) was greater than one for both resins, which indicated favorable sorption because n is a constant that represents the mutual interactions of sorbed species. Experimental values of n are usually greater than one, which indicates that the forces between the sorbed molecules are repulsive. In addition, Freundlich sorption n values closer to zero indicate systems that are more heterogeneous [42].

Sorption isotherms can also be used to compare the sorptive capacities of resins for Co(II) ions. The Langmuir constant, q_m, represents the ultimate sorption capacity when the surface is saturated with metal ions. The maximum sorption capacities, q_m, were 24.68 and 19.78 mg/g for the Amberlite 200C and Dowex 88 resins, respectively. Due to its smaller particle size, Amberlite 200C may have a higher sorption capacity than Dowex 88. In addition, the supplier indicated that the total exchange capacities of the Amberlite 200C and Dowex 88 resins are 1.7 and 1.8 eq/L (50 and 53 mg/g), respectively. In this study, the maximum sorption capacities of the Amberlite 200C and Dowex 88 resins were lower than the theoretic values given by the resin producers. This difference could result from differences in experimental conditions. Table 3 also presents a comparison of the sorption capacities of the resins [16]. Both resins are significant and have comparable sorption capacities relative to

Table 2
Estimated parameters of the Langmuir, Freundlich, Redlich–Peterson, and Temkin models at 25˚C

Isotherm	Type of resin	Isotherm parameters			R^2	S
		q_m (mg/g)	K (L/mg)			
Langmuir	Amberlite 200C	24.687	0.031		0.985	0.958
	Dowex 88	19.784	0.048		0.990	0.767
		n	K_f (mg/g)(L/mg)$^{1/n}$			
Freundlich	Amberlite 200C	1.862	1.878		0.991	0.731
	Dowex 88	2.165	2.110		0.967	1.403
		K_R (L/g)	a_R (L/mg)$^{\beta}$	β		
Redlich–Peterson	Amberlite 200C	41.633	19.801	0.5	0.990	0.764
	Dowex 88	1.095	0.087	0.9	0.988	0.863
		K_T (L/mg)	B			
Temkin	Amberlite 200C	3.415	2.403		0.895	2.459
	Dowex 88	1.040	3.274		0.953	1.654

the other resins, which indicate that Amberlite 200C and Dowex 88 could be valuable alternatives for treating industrial effluents.

3.4. Effects of temperature on cobalt ion sorption and thermodynamic parameters

The effects of temperature on the sorption of cobalt ions onto resins are shown in Fig. 5(a) and (b). The equilibrium experiments performed at different temperatures indicated that heavy metal ion sorption increased with increasing temperature. Increasing the temperature is known to increase the rate of diffusion across the external boundary layer and in the internal pores of the sorbent because the viscosity of the solution decreases [48–50].

Thermodynamically, parameters—such as the distribution coefficient (K_d), free energy change (ΔG°), enthalpy change (ΔH°), and entropy change (ΔS°)—can be calculated using classical thermodynamic equations [31,51–54].

The distribution coefficient (K_d, L/g) of metal ions between the aqueous phase and the resin phase at 25, 35, and 45°C is calculated as follows [43]:

$$K_d = \frac{(C_0 - C_e)V}{C_e M} \tag{8}$$

$$K_d = \frac{q_e}{C_e} \tag{9}$$

where C_0 and C_e are the initial and equilibrium concentrations of cobalt in solution, respectively, in mg/L, V is the volume of solution in L, and M is the mass of resins in g.

Table 3
Comparison of maximum sorption capacities of Co(II) by various sorbents

Resin	q_m (mg/g)	
IRN77 cation-exchange resin	86.2	[4]
SKN1 cation-exchange resin	69.4	[4]
Modified magnetic chitosan chelating resin	53.51	[6]
Lewatit MonoPlus SP 112	21.93	[21]
TVEX–PHOR	8.7	[43]
Amberlite IR-120 strong acid resin	40.1	[44]
Amberlite IRN-77 strong acid resin	74.6	[45]
Purolite S950 chelating resin	9.0	[46]
IDA chelating resin (CR-10)	138.5	[47]
IDA chelating resin (CR-15)	116.7	[47]
Amberlite 200C (this study)	24.68	
Dowex 88 (this study)	19.78	

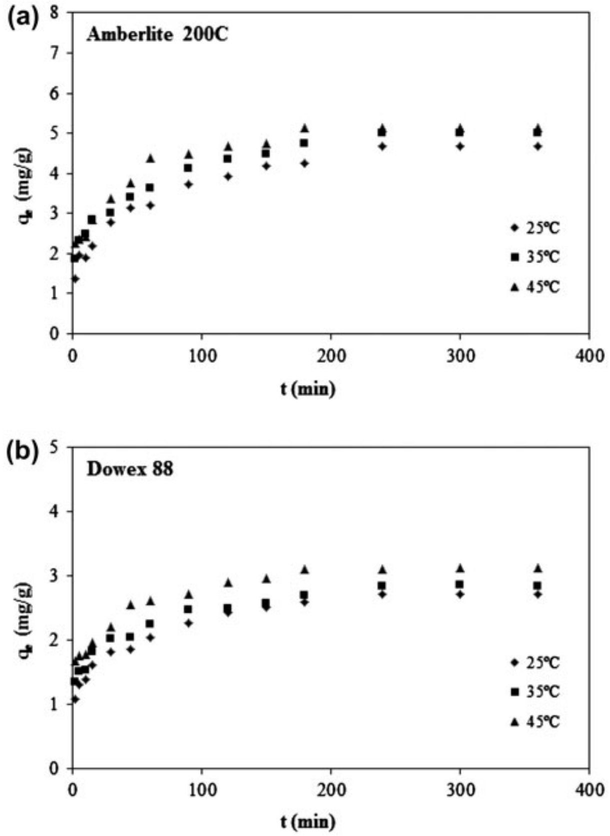

Fig. 5. The effects of temperature on the sorption of cobalt ions onto Amberlite 200C (a) and Dowex 88 (b).

The sorption free energy change, ΔG°, is known by Eq. (10).

$$\Delta G^\circ = -RT \ln K_d \tag{10}$$

Because ΔG° is given as kJ/mol, the distribution coefficient (K_d) in Eq. (10) is dimensionless [55–57]. If sorption occurs from the aqueous solution, K_d can be easily and simply recalculated as dimensionless by multiplying it by 1,000 (1 L = 1,000 mL or g, because the solution density is ≈1 g/mL).

Taking into account the last consideration, the ΔG° value is expressed as follows in Eq. (11):

$$\Delta G^\circ = -RT \ln 1{,}000 K_d \tag{11}$$

The relationships between ΔG°, ΔH°, and ΔS° can be expressed by the following equation [51]:

$$\Delta G^\circ = \Delta H^\circ - T\Delta S^\circ \tag{12}$$

To determine ΔH° and ΔS°, Eq. (13) can be used.

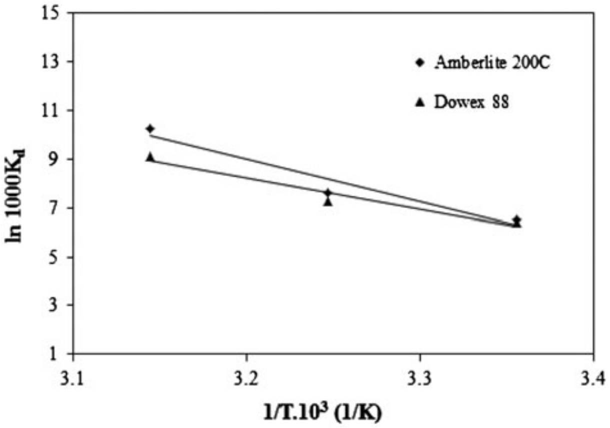

Fig. 6. Plots of ln K_d vs. $1/T$ for estimating the thermodynamic parameters for Co(II) sorption. Conditions: initial metal ion concentration: 100 mg/L; contact time: 240 min; sorbent dose: 20 g/L; pH 5.7.

$$\ln 1,000K_d = \Delta S^{\circ}/R - \Delta H^{\circ}/RT \tag{13}$$

The values of ΔH° and ΔS° were determined from the slope and intercept of the linear plot of ln 1,000 K_d vs. $1/T$ (Fig. 6), respectively. The Gibbs free energy (ΔG°) values were calculated using Eq. (11). As shown in Table 4, the values of ΔH° and ΔS° for Co(II), are 0.145 kJ/mol and 0.539 kJ/mol K, respectively, for Amberlite 200C and 0.107 kJ/mol and 0.411 kJ/mol K, respectively, for Dowex 88. The positive ΔH° values indicate that these processes are endothermic, which is supported by the increase in the uptake capacity of the sorbent with increasing temperature [51]. In addition, the positive ΔH° value suggests that physio-sorption occurs rather than chemisorption because ΔH° is less than 40 kJ/mol [5]. Furthermore, the ΔS° values were positive due to the exchange of the metal ions with more mobile ions on the resins, which resulted in greater entropy during the sorption process [23]. The magnitude of ΔG° decreased as the temperature increased, which indicated that the sorption of Co(II) ions for both resins is favorable at high temperatures. The negative values of ΔG° at each temperature confirm that the sorption of Co(II) ions was spontaneous and feasible. This type of behavior (low positive values of ΔH° and ΔS°, and negative values of ΔG°) has also been observed in earlier investigations of the sorption of cobalt onto sepiolite [26] and activated carbon derived from date seeds [5], and the sorption Cr(III) onto bentonite clay [58].

3.5. Sorption kinetics

To determine the mechanisms of the sorption process, four types of kinetic models were used to test the experimental data: pseudo-first-order, pseudo-second-order, intraparticle diffusion, and liquid film diffusion.

The pseudo-first-order rate equation is the most popular kinetic equation developed by Lagergren [32]. This model is based on the assumption that the sorption rate is determined by the number of sorption sites on the sorbent surface. The linear form is as follows [3,59]:

$$\ln(q_e - q_t) = \ln q_e - k_1 t \tag{14}$$

where q_t (mg/g) is the amount of Co(II) sorbed in time t (min); k_1 is the rate constant of the equation (1/min); and q_e is the amount of Co(II) at sorption equilibrium (mg/g). The sorption rate constant k_1 can be determined experimentally by plotting $\ln(q_e - q_t)$ vs. t (not shown).

A pseudo-second-order model was proposed by Ho and McKay [60] based on the following equation [31,61]:

$$t/q_t = 1/k_2 q_e^2 + t/q_e \tag{15}$$

where k_2 (g/mg min) is the rate constant of the second-order equation, q_t (mg/g) is the amount of Co(II) sorbed in time t (min), and q_e is the amount of Co(II) at sorption equilibrium (mg/g). In addition, k_2 and q_e can be calculated by plotting t/q_t against t (Fig. 7).

The values of different parameters determined from different kinetic models with correlation coefficients (R^2) and *SSE* values are presented in Tables 5 and 6. High correlation coefficients and low *SSE* values indicate the applicability of the pseudo-second-order model for describing the sorption process for both resins. In addition, the q_e value estimated by the pseudo-second-order model agrees with the experimental value of q_e, and the q_e values of the pseudo-first-order model were significantly lower than the experimental values. This result implies that the sorption data fit the pseudo-second-order kinetic model at all time intervals [32].

The pseudo-second-order model was applied to several sorption systems and, in many cases, this model provided better results for Co(II) sorption on natural hemp fibers [16], modified magnetic chitosan chelating resin [6], zeolite 13x [52], palygorskite [24] and Lewatit Monoplus SP 112 [21].

In general, the following phenomena are involved in sorption systems:

Table 4
Thermodynamic parameters calculated for the sorption of Co(II) at various temperatures

Resin	ΔG° (kJ/mol) 298 K	308 K	318 K	ΔH° (kJ/mol)	ΔS° (kJ/mol K)
Amberlite 200C	−16.17	−19.53	−27.04	0.145	0.539
Dowex 88	−15.79	−18.61	−24.08	0.107	0.411

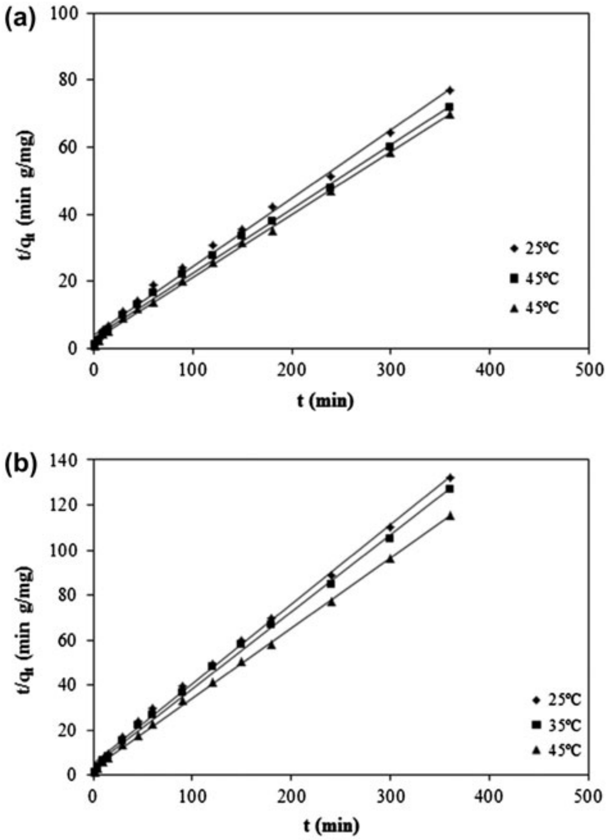

Fig. 7. Plots of the pseudo-second-order model for Co(II) sorption on Amberlite 200C (a) and Dowex 88 (b) at different temperatures. Conditions: initial metal ion concentration: 100 mg/L; sorbent dose: 20 g/L; pH 5.7.

(1) diffusion of metal ions from the bulk solution to a thin liquid layer that surrounds each particle,
(2) mass transfer from the fluid phase to the particle surface across the boundary layer (liquid–film diffusion),
(3) diffusion within the porous particle (diffusion within the particle or pore diffusion), and
(4) sorption onto the sorbent surface [62,63].

To determine whether intraparticle diffusion or film diffusion are rate-limiting steps, the sorption kinetic data were further analyzed.

Intraparticle diffusion can be estimated by the Weber and Morris model as follows [64]:

$$q_t = k_{\mathrm{id}} t^{1/2} \tag{16}$$

where q_t (mg/g) is the amount of Co(II) sorbed in time t (min) and k_{id} (mg/g min$^{1/2}$) is the intraparticle diffusion coefficient. These values can be found by plotting q_t vs. $t^{1/2}$ (Fig. 8). If the Weber–Morris plot of q_t vs. $t^{1/2}$ provides a straight line that passes through the origin, then the sorption process is only controlled by intraparticle diffusion [32,63,65].

The liquid film diffusion equation is as follows [38,66]:

$$-\ln(1 - F) = k_{\mathrm{fd}} t \tag{17}$$

where F is the fractional attainment of equilibrium $F = (q_t/q_e)$ and k_{fd} (1/min) is the liquid film diffusion coefficient. In addition, k_{fd} can be calculated by plotting $-\ln(1-F)$ vs. t (Fig. 9). A linear plot of $-\ln(1-F)$ against t with an intercept of zero would suggest that the sorption process was controlled by liquid film diffusion.

Figs. 8 and 9 show that both diffusion models were nearly linear for both resins, with correlation coefficients >0.90. However, none of the straight lines passed through the origin, which indicated some degree of boundary layer control [67–70]. Furthermore, these plots indicated that intraparticle diffusion and film diffusion are both rate-limiting steps for cobalt sorption onto Amberlite 200C and Dowex 88 resins [62]. Due to the values of k_{id} shown in Tables 5 and 6, cobalt molecules diffuse more rapidly on the surface of Amberlite 200C than on the surface of Dowex 88.

The magnitude of the activation energy (E_a) can indicate whether the sorption process is physical or chemical, and was calculated using the Arrhenius equation.

Table 5
Comparison of pseudo-first-order, pseudo-second-order, intraparticle diffusion, and liquid film diffusion kinetic constants, and calculated and experimental q_e values for Amberlite 200C

		Pseudo-first-order				Pseudo-second-order				Intraparticle diffusion			Liquid film diffusion		
T (K)	$q_{e(exp)}$ (mg/g)	k_1 (1/min)	$q_{e(cal)}$ (mg/g)	R^2	SSE	k_2 (g/mg min)	$q_{e(cal)}$ (mg/g)	R^2	SSE	k_{id} (mg/g min$^{1/2}$)	R^2	SSE	k_{fd} (1/min)	R^2	SSE
298	4.68	0.011	2.912	0.982	0.272	0.010	4.897	0.995	0.114	0.193	0.938	1.987	0.011	0.982	0.238
308	5.01	0.013	2.885	0.987	0.897	0.012	5.211	0.996	0.086	0.184	0.943	1.864	0.012	0.987	0.162
318	5.13	0.015	2.746	0.949	1.036	0.015	5.319	0.998	0.072	0.185	0.881	2.568	0.015	0.949	0.365

Table 6
Comparison of pseudo-first-order, pseudo-second-order, intraparticle diffusion, and liquid film diffusion kinetic constants, and calculated and experimental q_e values for Dowex 88

		Pseudo-first-order				Pseudo-second-order				Intraparticle diffusion			Liquid film diffusion		
T (K)	$q_{e(exp)}$ (mg/g)	k_1 (1/min)	$q_{e(cal)}$ (mg/g)	R^2	SSE	k_2 (g/mg min)	$q_{e(cal)}$ (mg/g)	R^2	SSE	k_{id} (mg/g min$^{1/2}$)	R^2	SSE	k_{fd} (1/min)	R^2	SSE
298	2.71	0.014	1.505	0.994	0.105	0.025	2.818	0.997	0.024	0.096	0.927	2.697	0.014	0.994	0.017
308	2.84	0.012	1.338	0.973	1.515	0.028	2.920	0.997	0.016	0.089	0.927	2.795	0.012	0.973	1.357
318	3.10	0.016	1.424	0.985	0.698	0.033	3.199	0.999	0.001	0.092	0.890	3.434	0.016	0.985	0.245

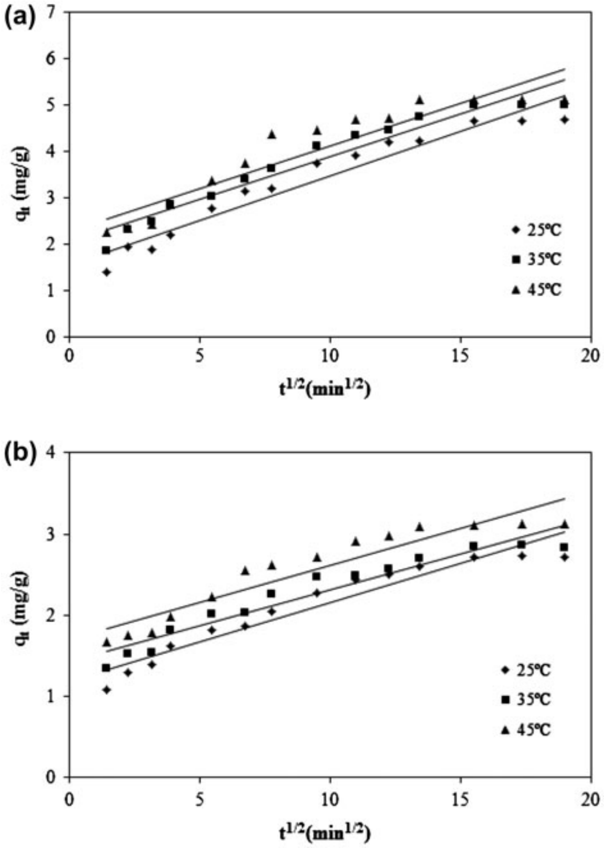

Fig. 8. Plots of intraparticle diffusion model for Co(II) sorption on Amberlite 200C (a) and Dowex 88 (b) at different temperatures. Conditions: initial metal ion concentration: 100 mg/L; sorbent dose: 20 g/L; pH 5.7.

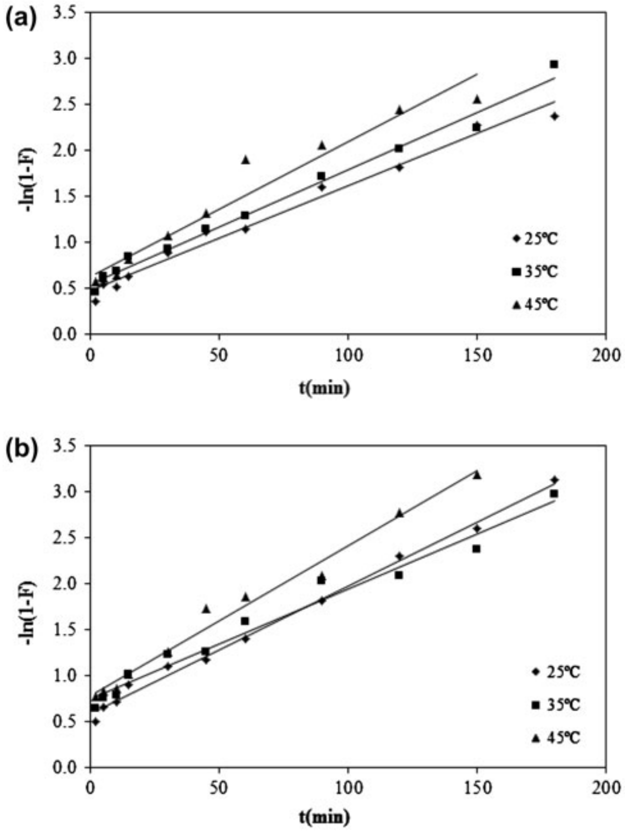

Fig. 9. Plots of the liquid film diffusion model for Co(II) sorption on Amberlite 200C (a) and Dowex 88 (b) at different temperatures. Conditions: initial metal ion concentration: 100 mg/L; sorbent dose: 20 g/L; pH 5.7.

$$\ln k = \ln A - E_a/RT \tag{18}$$

where E_a is the Arrhenius activation energy for the sorption process and indicates the minimum energy that reactants must have for the reaction to proceed, A is the Arrhenius factor, k is the sorption rate constant, and T is the solution temperature. The k value of the Arrhenius equation was obtained from the rate constant (k_2) of the pseudo-second-order equation. The ln k value was calculated at three different temperatures (25, 35, and 45°C), and ln k was plotted against $1/T$ (Fig. 10). This plot shows a straight line with a slope of $-E_a/R$ and an intercept of ln A. The Arrhenius activation energies calculated from the slope were 15.95 and 10.91 kJ/mol for Amberlite 200C and Dowex 88, respectively. The obtained activation energy values confirmed that the primary sorption mechanism of both resins is physical sorption. The physisorption process generally has energies of between 5 and 40 kJ/mol, while the chemisorption process has a higher activation energy (40–800 kJ/mol) [71]. In addition, when the activation energy is low, the rate is controlled by diffusion mechanisms [72]. The positive

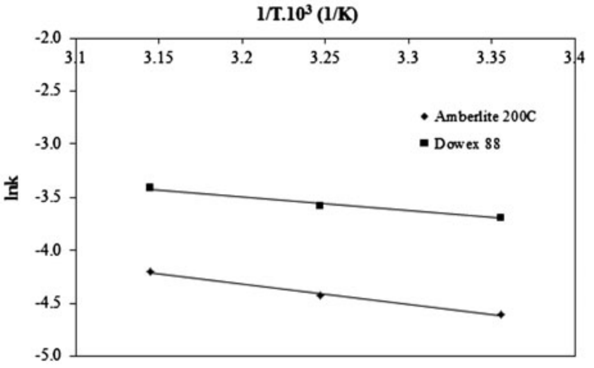

Fig. 10. Arrhenius equation plots for the sorption of Co(II). Conditions: initial metal ion concentration: 100 mg/L; sorbent dose: 20 g/L; pH 5.7.

Table 7
Desorption data for Co(II) on resins

Desorption %			
	Concentration (M)	Amberlite 200C	Dowex 88
HCl	0.5	22.75	18.95
	1.0	53.70	51.84
	2.0	96.80	73.76
HNO_3	0.5	17.05	14.24
	1.0	40.48	39.02
	2.0	75.63	67.10
H_2SO_4	0.5	27.02	36.08
	1.0	68.67	51.86
	2.0	100.00	86.06

values of E_a also suggest that increases in temperature favor sorption and that the sorption process is an endothermic process in nature [51].

3.6. Metal desorption

To make the sorption process more economical by repeatedly using the sorbent [49], the desorption potential of the resins was investigated. Desorption studies were carried out in HCl, NaOH, HNO_3 and H_2SO_4 solutions at various concentrations to remove metals that were sorbed onto the resins. The systematic influences of these desorbing solutions on the amounts of metal sorbed to the resins are shown in Table 7.

Amberlite 200C showed the highest desorption efficiencies of 96.8 and 100% when using 2 M HCl and 2 M H_2SO_4, respectively, which resulted in lower desorption efficiencies for Dowex 88. When using 2 M HNO_3, only 75.63 and 67.1% of Co(II) were desorbed from the Amberlite 200C and Dowex 88, respectively. However, the desorption attempts were unsuccessful for both resins when using NaOH, and the desorption efficiencies increased as the acid concentrations increased. These results suggest that leaching conditions significantly affect the efficiency of metal desorption from the resins studied in this work.

4. Conclusions

In this study, the sorption of Co(II) on Amberlite 200C and Dowex 88 resins was investigated using batch tests by varying experimental conditions, such as the pH of the solution, the resin dose, and the temperature of the solution. The solution pH was the most important parameter that affected sorption and the most effective pH for cobalt removal was between pH 4–8 for both resins. The batch equilibrium results suggested that the sorption process followed a pseudo-second-order kinetic model for both resins. The Langmuir, Freundlich, Redlich–Peterson, and Temkin sorption models were used to mathematically describe the sorption of Co(II) ions onto the resins. For the Dowex 88 resin, the sorption process followed the Langmuir isotherm, and for the Amberlite 200C resin, the sorption process followed the Freundlich isotherm. When comparing the sorption capacities obtained from the Langmuir isotherm model, the Amberlite 200C resin had a higher sorption capacity than the Dowex 88 resin.

The positive enthalpy change indicated that the sorption process was endothermic for both resins. The negative ΔG° values indicated that the sorption of Co(II) ions was spontaneous for both resins. Additionally, activation energies confirmed that the sorption process was physical for both resins.

The results from the 2 M H_2SO_4 desorption experiments showed that the Co(II) sorbed by the Amberlite 200C resins can easily be desorbed (100%), whereas the Co(II) sorbed onto Dowex 88 was not removed as efficiently (86%). Overall the results implied that Amberlite 200C had a better sorption and regeneration capacity than Dowex 88, which indicated that Amberlite 200C may be preferred for removing and recovering cobalt ions. The results of this study may be useful when treating wastewaters containing heavy metal ions.

Acknowledgment

The authors wish to thank Eskisehir Osmangazi University Scientific Research Projects Commission for partially supporting this study financially (project no.200815001).

References

[1] E.A. Deliyanni, E.N. Peleka, K.A. Matis, Removal of zinc ion from water by sorption onto iron-based nanoadsorbent, J. Hazard. Mater. 141 (2007) 176–184.
[2] F. Gode, E. Pehlivan, A comparative study of two chelating ion-exchange resins for the removal of chromium(III) from aqueous solution, J. Hazard. Mater. 100 (2003) 231–243.
[3] B. Alyüz, S. Veli, Kinetics and equilibrium studies for the removal of nickel and zinc from aqueous solutions by ion exchange resins, J. Hazard. Mater 167 (2009) 482–488.
[4] S. Rengaraj, S.H. Moon, Kinetics of adsorption of Co(II) removal from water and wastewater by ion exchange resins, Water Res. 36 (2002) 1783–1793.
[5] I.H. Aljundi, S.K. Al-Dawery, Equilibrium and thermodynamic study of cobalt adsorption on activated carbon derived from date seeds, Desalin. Water Treat. 52 (2014) 4830–4836.

[6] M. Monier, D.M. Ayad, Y. Wei, A.A. Sarhan, Adsorption of Cu(II), Co(II), and Ni(II) ions by modified magnetic chitosan chelating resin, J. Hazard. Mater. 177 (2010) 962–970.

[7] Water Pollution Control Regulation of Turkey, Technical Procedure Notification, 1991.

[8] S.S. Al-Shahrani, Treatment of wastewater contaminated with cobalt using Saudi activated bentonite, Alexandria Eng. J. 53 (2014) 205–211.

[9] M.A. Khan, W. Jung, O. Kwon, Y.M. Jung, K. Paeng, S. Cho, B. Jeon, Sorption studies of manganese and cobalt from aqueous phase onto alginate beads and nano-graphite encapsulated alginate beads, J. Ind. Eng. Chem. 20 (2014) 4353–4362.

[10] H. Yüzer, M. Kara, E. Sabah, M.S. Celik, Contribution of cobalt ion precipitation to adsorption in ion exchange dominant systems, J. Hazard. Mater. 151 (2008) 33–37.

[11] F.L. Becker, D. Rodríguez, M. Schwab, Magnetic removal of cobalt from waste water by ferrite co-precipitation, Procedia Mater. Sci. 1 (2012) 644–650.

[12] S. Bouranene, P. Fievet, A. Szymczyk, M.E. El-Hadi Samar, A. Vidonne, Influence of operating conditions on the rejection of cobalt and lead ions in aqueous solutions by a nanofiltration polyamide membrane, J. Membr. Sci. 325 (2008) 150–157.

[13] C. Cojocaru, G. Zakrzewska-Trznadel, A. Jaworska, Removal of cobalt ions from aqueous solutions by polymer assisted ultrafiltration using experimental design approach. Part 1: Optimization of complexation conditions, J. Hazard. Mater. 169 (2009) 599–609.

[14] A. Shafaei, E. Pajootan, M. Nikazar, M. Arami, Removal of Co(II) from aqueous solution by electrocoagulation process using aluminum electrodes, Desalination 279 (2011) 121–126.

[15] Sh.M. Yu, A.P. Ren, ChL Chen, Y.X. Chen, X. Wang, Effect of pH, ionic strength and fulvic acid on the sorption and desorption of cobalt to bentonite, Appl. Radiat. Isot. 64 (2006) 455–461.

[16] L. Tofan, C. Teodosiu, C. Paduraru, R. Wenkert, Cobalt(II) removal from aqueous solutions by natural hemp fibers: Batch and fixed-bed column studies, Appl. Surf. Sci. 285 (2013) 33–39.

[17] N. Dizge, B. Keskinler, H. Barlas, Sorption of Ni(II) ions from aqueous solution by Lewatit cation-exchange resin, J. Hazard. Mater. 167 (2009) 915–926.

[18] F.D. Mendes, A.H. Martins, Selective sorption of nickel and cobalt from sulphate solutions using chelating resins, Int. J. Miner. Process. 74 (2004) 359–371.

[19] X. Chun-Hua, F. Yu-Jie, C.-P. Yao, S. Chen, Removal of Co(II) from aqueous solutions by NKC-9 resin, Trans. Nonferrous Met. Soc. China 20 (2010) 1141–1147.

[20] M. Monier, D.M. Ayad, Y. Wei, A.A. Sarhan, Preparation and characterization of magnetic chelating resin based on chitosan for adsorption of Cu(II), Co(II), and Ni(II) ions, React. Funct. Polym. 70 (2010) 257–266.

[21] Y. Aşçı, Ş. Kaya, Removal of cobalt ions from water by ion-exchange method, Desalin. Water Treat. 52 (2014) 267–273.

[22] R.R. Bhatt, B.A. Shah, Sorption studies of heavy metal ions by salicylicacid-formaldehyde-catechol terpolymeric resin: Isotherm, kinetic and thermodynamics, Arab. J. Chem. 8 (2015) 414–426.

[23] B. Esma, A. Omar, D.M. Amine, Comparative study on lanthanum(III) sorption onto Lewatit TP 207 and Lewatit TP 260, J. Radioanal. Nucl. Chem. 299 (2014) 439–446.

[24] M. He, Y. Zhu, Y. Yang, B. Han, Y. Zhang, Adsorption of cobalt(II) ions from aqueous solutions by palygorskite, Appl. Clay Sci. 54 (2011) 292–296.

[25] P. Thilagavathy, T. Santhi, Kinetics, isotherms and equilibrium study of Co(II) adsorption from single and binary aqueous solutions by *Acacia nilotica* leaf carbon, Chin. J. Chem. Eng. 22 (2014) 1193–1198.

[26] M. Kara, H. Yuzer, E. Sabah, M.S. Celik, Adsorption of cobalt from aqueous solutions onto sepiolite, Water Res. 37 (2003) 224–232.

[27] K.A. Krishnan, T.S. Anirudhan, Kinetic and equilibrium modelling of cobalt(II) adsorption onto bagasse pith based sulphurised activated carbon, Chem. Eng. J. 137 (2008) 257–264.

[28] Y.K. Kım, K.J. Lee, Synthesis of a magnetic composite resin and its cobalt removal characteristics in aqueous solution, J. Nucl. Sci. Technol. 38 (2001) 785–792.

[29] N.V. Nguyen, J. Jeong, M.K. Jha, J. Lee, K. Osseo-Asare, Comparative studies on the adsorption of Au(III) from waste rinse water of semiconductor industry using various resins, Hydrometallurgy 105 (2010) 161–167.

[30] Y. Bulut, H. Aydın, A kinetics and thermodynamics study of methylene blue adsorption on wheat shells, Desalination 194 (2006) 259–267.

[31] S. Edebali, E. Pehlivan, Evaluation of Amberlite IRA96 and Dowex 1×8 ion-exchange resins for the removal of Cr(VI) from aqueous solution, Chem. Eng. J. 161 (2010) 161–166.

[32] Y. Bao, F. Yuan, X. Zhao, Q. Liu, Y. Gao, Equilibrium and kinetic studies on the adsorption debittering process of ponkan (*Citrus reticulata* Blanco) juice using macroporous resins, Food Bioprod. Process. 94 (2015) 199–207.

[33] L. Langmuir, The constitution and fundamental properties of solids and liquids, J. Am. Chem. Soc. 38 (1916) 2221–2295.

[34] R. Han, J. Zhang, P. Han, Y. Wang, Z. Zhao, M. Tang, Study of equilibrium, kinetic and thermodynamic parameters about methylene blue adsorption onto natural zeolite, Chem. Eng. J. 145 (2009) 496–504.

[35] E. Pehlivan, S. Cetin, Sorption of Cr(VI) ions on two Lewatit-anion exchange resins and their quantitative determination using UV–visible spectrophotometer, J. Hazard. Mater. 163 (2009) 448–453.

[36] Y. Aşçı, M. Nurbaş, Y. Sağ Açıkel, A comparative study for the sorption of Cd(II) by K-feldspar and sepiolite as soil components, and the recovery of Cd(II) using rhamnolipid biosurfactant, J. Environ. Manage. 88 (2008) 383–392.

[37] O. Redlich, D.L. Peterson, A useful adsorption isotherm, J. Phys. Chem. 63 (1959) 1024–1029.

[38] S. Rengaraj, J. Yeon, Y. Kim, Y. Jung, Y. Ha, W. Kim, Adsorption characteristics of Cu(II) onto ion exchange resins 252H and 1500H: Kinetics, isotherms and error analysis, J. Hazard. Mater. 143 (2007) 469–477.

[39] W. Shao, X. Li, Q. Cao, F. Luo, J. Li, Y. Du, Adsorption of arsenate and arsenite anions from aqueous medium by using metal(III)-loaded amberlite resins, Hydrometallurgy 91 (2008) 138–143.

[40] A. Deepatana, M. Valix, Comparative adsorption isotherms and modeling of nickel and cobalt citrate complexes onto chelating resins, Desalination 218 (2008) 334–342.

[41] S. Shahmohammadi-Kalalagh, H. Babazadeh, A.H. Nazemi, M. Manshouri, Isotherm and kinetic studies on adsorption of Pb, Zn and Cu by kaolinite, Caspian J. Environ. Sci. 9 (2011) 243–255.

[42] Y. Aşçı, M. Nurbaş, Y. Sağ Açıkel, A comparative study for the sorption of Cd(II) by soils with different clay contents and mineralogy and the recovery of Cd(II) using rhamnolipid biosurfactant, J. Hazard. Mater. 154 (2008) 663–673.

[43] S.I. El-Dessouky, E.A. El-Sofany, J.A. Daoud, Studies on the sorption of praseodymium(III), holmium(III) and cobalt(II) from nitrate medium using TVEX–PHOR resin, J. Hazard. Mater. 143 (2007) 17–23.

[44] R.S. Juang, S.H. Lin, T.Y. Wang, Removal of metal ions from the complexed solutions in fixed bed using a strong-acid ion exchange resin, Chemosphere 53 (2003) 1221–1228.

[45] S.Y. Kang, J.U. Lee, S.H. Moon, K.W. Kim, Competitive adsorption characteristics of Co^{2+}, Ni^{2+}, and Cr^{3+} by IRN-77 cation exchange resin in synthesized wastewater, Chemosphere 56 (2004) 141–147.

[46] A. Deepatana, M. Valix, Recovery of nickel and cobalt from organic acid complexes: Adsorption mechanisms of metal-organic complexes onto aminophosphonate chelating resin, J. Hazard. Mater. 137 (2006) 925–933.

[47] E.S. Dragan, M.V. Dinu, G. Lisa, A.W. Trochimczuk, Study on metal complexes of chelating resins bearing iminodiacetate groups, Eur. Polym. J. 45 (2009) 2119–2130.

[48] T.Y. Kim, S.S. An, W.G. Shim, J.W. Lee, S.Y. Cho, J.H. Kim, Adsorption and energetic heterogeneity properties of cesium ions on ion exchange resin, J. Indust. Eng. Chem. 27 (2015) 260–267.

[49] Y. Zhang, Y. Li, L. Yang, X. Ma, L. Wang, Z. Ye, Characterization and adsorption mechanism of Zn^{2+} removal by PVA/EDTA resin in polluted water, J. Hazard. Mater. 178 (2010) 1046–1054.

[50] M. Dogan, M. Alkan, A. Türkyilmaz, Y. Özdemir, Kinetics and mechanism of removal of methylene blue by adsorption onto perlite, J. Hazard. Mater. 109 (2004) 141–148.

[51] Z. Yua, T. Qia, J. Qu , L. Wang, J. Chu, Removal of Ca(II) and Mg(II) from potassium chromate solution on Amberlite IRC 748 synthetic resin by ion exchange, J. Hazard. Mater. 167 (2009) 406–412.

[52] Y. Jin, Y. Wu, J. Cao, Y. Wu, Adsorption behavior of Cr(VI), Ni(II), and Co(II) onto zeolite 13x, Desalin. Water Treat. 54 (2015) 511–524.

[53] R. Donat, A. Akdogan, E. Erdem, H. Cetisli, Thermodynamics of Pb^{2+} and Ni^{2+} adsorption onto natural bentonite from aqueous solutions, J. Colloid Interf. Sci. 286 (2005) 43–52.

[54] Y. Zheng, C. Xiong, C. Yao, F. Ye, J. Jiang, X. Zheng, Q. Zheng, Adsorption performance and mechanism for removal of Cd(II) from aqueous solutions by D001 cation-exchange resin, Water Sci. Technol. 69 (2014) 833–839.

[55] S.K. Milonjic, A consideration of the correct calculation of thermodynamic parameter of adsorption, J. Serb. Chem. Soc. 72(12) (2012) 1363–1367.

[56] F.A. Bertoni, A.C. Medeot, J.C. Gonzalez, L.F. Sala, S.E. Bellu, Application of green seaweed biomass for MoVI sorption from contaminated waters. Kinetic, thermodynamic and continuous sorption studies, J. Colloid Interf. Sci. 446 (2015) 122–132.

[57] P. Sharma, B.K. Saikia, M.R. Das, Removal of methyl green dye molecule from aqueous system usingreduced graphene oxide as an efficient adsorbent: Kinetics, isothermand thermodynamic parameters, Colloids Surf., A 457 (2014) 125–133.

[58] S.S. Tahir, R. Naseem, Removal of Cr(III) from tannery wastewater by adsorption onto bentonite clay, Sep. Purif. Technol. 53 (2007) 312–321.

[59] K.S. Rao, G.R. Chaudhury, B.K. Mishra, Kinetics and equilibrium studies for the removal of cadmium ions from aqueous solutions using Duolite ES 467 resin, Intl. J. Miner. Process 97 (2010) 68–73.

[60] Y.S. Ho, G. McKay, Pseudo-second order model for sorption processes, Process Biochem. 34 (1999) 451–465.

[61] X. Pan, J. Wang, D. Zhang, Sorption of cobalt to bone char: Kinetics, competitive sorption and mechanism, Desalination 249 (2009) 609–614.

[62] W. Zhang, C. Hong, B. Pan, Z. Xu, Q. Zhang, Q. Zhang, A comparative study of the adsorption properties of 1-naphthylamine by XAD-4 and NDA-150 polymer resins, Colloids Surf., A 331 (2008) 257–262.

[63] G. Darracq, J. Baron, M. Joyeux, Kinetic and isotherm studies on perchlorate sorption by ion-exchange resins in drinking water treatment, J. Water Process Eng. 3 (2014) 123–131.

[64] W.J. Weber, J.C. Morris, Advances in water pollution research: Removal of biologically-resistent pollutants from waste waters by adsorption, in: Proceedings of the International Conference on Water Pollution Symposium, vol. 2, Pergamon Press, Oxford, 1962, pp. 231–266.

[65] Y. Aşçı, Ü Açıkel, Y. Sağ Açıkel, Equilibrium, hysteresis and kinetics of cadmium desorption from sodium-feldspar using rhamnolipid biosurfactant, Environ. Technol. 33 (2012) 1857–1868.

[66] K. Fujiwara, A. Ramesh, T. Maki, H. Hasegawa, K. Ueda, Adsorption of platinum (IV), palladium (II) and gold(III) from aqueous solutions onto l-lysine modified crosslinked chitosan resin, J. Hazard. Mater. 146 (2007) 39–50.

[67] J. Zhang, C. Wu, A. Jia, B. Hu, Kinetics, equilibrium and thermodynamics of the sorption of p-nitrophenol on two variable charge soils of Southern China, Appl. Sur. Sci. 298 (2014) 95–101.

[68] E.S. Dragan, A.I. Cocarta, M.V. Dinu, Facile fabrication of chitosan/poly(vinyl amine) composite beads with enhanced sorption of Cu^{2+} Equilibrium, kinetics, and thermodynamics, Chem. Eng. J. 255 (2014) 659–669.

[69] V. Vadivelan, K.V. Kumar, Equilibrium, kinetics, mechanism, and process design for the sorption of methylene blue onto rice husk, J. Colloid Interf. Sci. 286 (2005) 90–100.

[70] M. Kapur, M.K. Mondal, Competitive sorption of Cu(II) and Ni(II) ions from aqueous solutions: Kinetics, thermodynamics and desorption studies, J. Taiwan Inst. Chem. Eng. 45 (2014) 1803–1813.

[71] S. Chakravarty, A. Mohanty, T. Nag Sudha, A.K. Upadhyay, J. Konar, J.K. Sircar, A. Madhukar, K.K. Gupta, Removal of Pb(II) ions from aqueous solution by adsorption using bael leaves (Aegle marmelos), J. Hazard. Mater. 173 (2010) 502–509.

[72] H. Scott Fogler, Elements of Chemical Reaction Engineering, Prentice-Hall Int. Inc. 1992.